QUANTIFICATION OF STANDING WAVE PATTERNS IN ROTATING FLEXIBLE DISKS USING OPTICAL REFLECTION TECHNIQUES

Yiping Ma

Iomega Corporation
Head & Media Group
Research and Development Division
1821 West Iomega Way
Roy, Utah 84067
(801)778-4640 (Tel)
(801)778-1030 (fax)

Fred C. Thomas III

Iomega Corporation
Advanced Product Development Group
Research and Development Division
1821 West Iomega Way
Roy, Utah 84067
(801)778-4662 (Tel)
(801)778-1030 (fax)

ABSTRACT

This paper is a follow-on to a paper previously presented to ASME on an experimental instrument designed to enable the observation of standing wave modes for flexible media. In that earlier paper qualitative results showing changes in the disk standing waves were obtained using the experimental setup. The current paper presents the same experimental system from the perspective of looking at the system as an optical instrument, and, based on optical ray trace methodology, quantifies the results seen in the previous paper on a more absolute basis. Based on this analysis, the authors also describe design changes from both an instrument setup perspective and the application of other electro-optic sensor technologies which will improve the system's static and dynamic resolution.

INTRODUCTION

Magnetic recording on flexible disks has been mostly limited to products that have low performance, low capacity and poor reliability, such as the standard 5.25 inch floppy drive and the 3.5 inch floppy drive. Both have capacity in the range of a few megabytes and average latency of more than 50 milliseconds due to slow rotational rates. For example, the ubiquitous 1.44 MB 3.5 inch floppy rotates at 300 rpm while other new flexible media disk storage technologies such as the LS-120® rotate at a rate of 720 RPM. This contrasts to rotational rates of 7200 rpm for high-end fixed disk storage products being produced today.

One of the limiting factors to obtaining higher performance from flexible media products is the complicated disk dynamics associated with the floppy disks at high rotational speeds. For a long period of time, the only commercially available high capacity and high performance disk drive product using flexible disks was the Bernoulli® drive. In this drive the flexible disk is rotated at 2363 rpm next to a stationary Bernoulli plate in order to impart media stability. Tight manufacturing tolerances and specially designed recording heads, however, continue to make the Bernoulli drive quite expensive.

The recent commercial success of the Zip™ drive has brought renewed interest in the study of flexible disk dynamics. In the Zip drive, a piece of 3.5 inch flexible media is stabilized by spinning it between two stationary plates at approximately 3000 rpm. A pair of slightly modified Winchester nano-sliders mounted on industry standard suspensions are arranged in a configuration which provides appropriate pinching force or gram load to adequately achieve low fly-height. Hence, due to what proved to be a very robust but straightforward method of media stabilization and a simple HDI design, the cost of manufacture for the Zip drive was made extremely low. The instrument described in this paper, the "Flexible Disk Mode Observer," in large part contributed to these achievements through the insights it provided into the dynamics of high rotational rate floppies.

Previously published studies of flexible media dynamics have mostly been analytical, and, as such, have been based on more idealized boundary conditions due to the complexity of the problem. Some of the earliest works were focused on the understanding of the free vibration of rotating disks (Lamb and Southwell, 1921, and Southwell, 1921). Some of the more recent works studied the vibration of a free spinning disk

under fixed point source loading (Benson and Bogy, 1978, Benson, 1983, and, Ono and Maeno, 1986). The importance of the disk bending stiffness and its analytical design implications were identified. A term called "foundation stiffness" was later introduced to the field to describe the effect of a plate placed next to a rotating disk (Adams, 1987). This is the primary mechanism that stabilizes the disk inside the Bernoulli drive. Some attempts were also made to study the mechanical interface between the recording head and flexible disk (Adams, 1980, and, Greenberg, 1978). These studies were mostly restricted to fixed spherical heads.

Studies with the "Flexible Disk Mode Observer," however, show the media dynamics to be of a complicated nonlinear form which makes complete and thorough numerical analysis very difficult. An empirical approach is therefore adopted here. Earlier experimental work, by other authors, using a 3.5 inch disk concentrated mostly on disk stabilization in the absence of the external head loading (Kitagawa, et. al., 1990). When the heads were loaded onto the disk, the authors only studied the very limited case of where the heads were fixed in radial position and penetration.

The recent experimental work of Ma and Jones provided some very interesting observations of the flexible disk standing waves phenomena for a 3.5 inch flexible disk spinning centrally between a pair of stationary plates at high rotational speed (3000 rpm to 4500 rpm) and while at the same time being under the load of suspended pinching nano-sliders. Such phenomena as standing wave phase shift, disk snap and disk bistable vibration were observed through the aid of the herein described instrument. The work, we believe, is significant because it addresses pertinent HDI issues related to the Zip drive. Figure 1 shows a typical example of standing wave topography observed. Although the initial work was quite insightful, it lacked numerical quantification of the visual results.

The intent of the present paper is to explain the operating theory of the instrument by examining it as an optical device, or system, and based on this understanding, quantify numerically some of the results previously presented.

EXPERIMENTAL TECHNIQUE

A summary review of the experimental approach taken, equipment involved and parameter space exploration possible with the "Flexible Disk Mode Observer" instrument is presented next.

Figure 2 illustrates the basic setup of the "Flexible Disk Mode Observer." It consists of a video camera, a light source, a light diffuser, a reference target, a spin stand with variable speed motor controller, a set of plates simulating cartridge housing, and a pair of 50% Winchester heads mounted on suspensions which are attached to a stage capable of moving in a radial direction relative to the spin axis.

The video camera is aligned with the center of the motor spindle and leveled with the motor datum surface. The light source and diffuser combination provide uniform illumination over the spin stand. The reference target or "structured mode pattern" is made of transparency film with a circular pattern opaquely printed on the film. This target is mounted in front of the light diffuser. Since the surface of flexible media is specularly reflective, the image of the "structured mode pattern" will be reflected by the flexible disk and observed by the video camera. Any distortion in the reflected image will indicate a deflection of the flexible disk from its nominal plane which is parallel to the plane containing the "structured mode pattern." This enables the observation of standing wave formations. To further facilitate observation, one of the "structured mode pattern" rings is a dashed line so that the distortion direction of the reflected rings may be ascertained. The reflected image which is distorted by the mode displacements of the media is captured electronically by the camera.

The flexible disk is rotated in the middle of a pair of flat plates with a radial cutout for head access. The plates are spaced 1.2 mm apart. The top plate is made of clear plastic to allow observation of the whole disk. The reflection off this clear plastic plate offers a visual reference of how an undistorted disk would appear.

The heads used are the standard 50% two-rail taper-flat Winchester-type heads. They are mounted on commonly used 50% Winchester suspensions. The head/suspension assembly is then attached to the arm of a rotary actuator. The rotary actuator is mounted on a stage that provides vertical, or Z, axis movement to simulate misalignment between the head stack assembly (HSA) and cartridge, hence changing head penetration. Head penetration is defined as the axial position difference between the static centerline of the head pair and centerplane of the disk at the hub. Head penetration is negative if the head pair centerline is lower than the centerplane of the disk.

This system provides one with the ability to explore flexible media standing wave dynamics as the result of changing various disk drive state space parameters. This would include using different head/suspension designs and combinations with a spectrum of different head gram-loads applied to the interface. The media state space explorable would include the varying of: substrate thickness, disk outer diameter, disk hubbing diameter, as well as different methods for hubbing. Refinement of media mode stabilization methods and the understanding of physical mode disrupters is also territory of significant interest that the "Flexible Disk Mode Observer" instrument provides clear and important empirical feedback about. For example, the effects of the shape of the head access slot were studied in detail using this system. With a particular head-to-disk interface (HDI) in place, as described substantially by the combination of parameters listed above, the researcher is then able to understand, and therefore tune their disk drive's

design relative to disk rotational rate requirements and head penetration tolerancing considerations.

OPTICAL SYSTEM QUANTIFICATION

The "Flexible Disk Mode Observer" instrument allows the flexible media researcher to observe mode dynamics of a rotating disk. Figure 3 illustrates in detail the optical layout these investigators have used to observe the standing wave mode dynamics of a 3.5 inch flexible disk. In essence, this optical mode observer technique uses the surface of the flexible media as a mirror to observe a fixed object, the "structured mode pattern." As seen in Fig. 8 and 9, a circular pattern concentric with the disk's center of rotation is used for these investigations. This type of pattern accentuates angular deformations in the media in the radial direction. Alternatively, a line pattern of spokes will accentuate circumferential deformations in the media. Displacements of these structured images is due to angular deformations in the media in a direction normal to the pattern's line edges.

The disk in this system is initially a flat mirror which makes the image of the "structured mode pattern" appear to come from behind the media. As the media deforms, while rotating, into various standing wave patterns, it acts as a deformable mirror or a dynamically changing "fun house" mirror. Just as one's image is distorted into skinny and fat profiles with reflections from a concave or convex "fun house" mirror, the original structured mode pattern being viewed with the video imaging system is distorted upon reflection from nonflat media. From these image distortions we are able to make a fairly good determination as to the media's angular attitude while spinning. As noted, the concentric circular pattern allows for measurement of the radial vector component of this distortion.

As noted in the Introduction, in order to make interpretation of the image distortion as easy as possible and not require digital image processing techniques, a thin, rigid and flat acrylic sheet was mounted in close proximity to the spinning disk. Although acrylic is highly optically transparent (92% for 1/8" thick piece) it has a surface reflectance of about 7%. This reflectance provides a nice fixed reference image of the "structured mode pattern" being observed on the disk. Relative displacements between this reference image and the disk's distorted reflected image allow for a simple means to measure and analyze media deformations.

System Geometric Optics

Since the flexible media acts as a mirror and as such light striking it obeys Fermat's law of reflection. This law tells us that the angle of reflection of a ray of light striking a surface is equal and opposite to the angle of incidence relative to a normal vector at the point of incidence on the surface. Equation 1 expresses this relation with the angular nomenclature being defined by Fig. 4.

$$\alpha_1 = \alpha_2 \tag{1}$$

From this simple relation we see that as the surface of the media takes on standing wave orientations which distort the surface from planar, the path of the light rays striking that distorted surface are altered upon reflection by an amount equal to twice the change in angular orientation of the media. This redirected ray if captured by the camera optical system's aperture, is displaced from its original location on the CCD imager plane, and is viewed as a displacement of the lines edge in the video display.

Figure 5 shows the geometrical relation between a change in the entrance angle of a ray of light into a lens and the displacement of that rays focal point on the image plane of the camera. This focal plane displacement (δ) may be calculated, to the first order, by the following relation:

$$\delta = \theta \times fl \tag{2}$$

Theta (θ) is in radians and the lens focal length (fl) along with the focal plane displacement are in similar units of length. A deformed area on the flexible media reflects a distorted image of the planar structured pattern. Displacements of a given point in this image pattern in the focal plane is simply the offset from that same point reflecting from the proximate, flat, acrylic surface.

In order to interpret structured line displacements from the acrylic reference planar line reflection as seen in the video monitor, an extension of Eq. 2 is formulated. This expression takes into account the format of the imager (size) being used as well as the format of the monitor being used. It is assumed that the aspect ratios of both are the same.

$$\beta = \frac{1}{2} \times \left[\frac{(\delta_{monitor} \times format_{imager})}{(fl \times format_{monitor})} \right] \times \frac{180}{\pi} \tag{3}$$

where, β (degrees) is the flexible media angle of distortion, $\delta_{monitor}$ (mm) is the displacement of line edge from the reference image edge (acrylic reflection), $format_{imager}$ (mm) is the diagonal measurement of CCD imager (e.g. 1/2" = 12.7mm),

$format_{monitor}$ (mm) is the diagonal measurement of monitor and fl (mm) is the focal length of the camera lens (eg 16 mm).

The steps required to obtain this new formulation include:
1) algebraically formulating θ of Eq. 2 as β, ($\beta=\delta/fl$);
2) accounting for the angle of reflection off the media being double the angle of deformation of the media due to Fermat's law (1/2 factor);
3) providing for the conversion of focal displacement as measured in the CCD image plane to that observed on the electronically magnified display monitor. this factor may also be described as the inverse of this electronic magnification ($format_{imager}/format_{monitor}$) and;
4) providing a radian-to-degree angular unit conversion ($180/\pi$).
With this new formulation, easily measured displacements of the "structured mode pattern" as viewed on the monitor can be directly converted to media angular deformations.

By substituting the full width of the monitor in for $d_{monitor}$, one can calculate the full horizontal field of view of one's imager. By dividing this number by the number of pixels in the horizontal direction of the CCD imager, one obtains a measure of the angular resolution of the mode observer instrument. For the standing wave mode observer used for these investigations we calculate the horizontal field of view to be 45.4 degrees with a pixel resolution of about 0.08 degrees. Hence, angularity changes in the media of 4.5 minutes will shift the edge of a line in the viewed "structured mode pattern" one pixel distance or, in this particular case, 16.6 microns at the imager plane of focus.

Reflective Blur Function

Next we look at the top half of Fig. 3 and trace through what happens to a ray of light leaving a defining feature on the object being imaged, the "structure mode pattern." A line edge in the circular pattern can be considered such a defining feature. The light leaving that line edge is emitted from the diffusely scattering opal plastic in what is called a lambertian manner. In Fig. 6 we see the hemispherical intensity profile for this type of source. As a result of this lambertian distribution, the line edge sends rays of light in all directions. The portion of this light which ends up being reimaged by the lens on the observing CCD imager is only that portion that hits the reflecting disk surface and gains entrance to the aperture stop of the camera.

Light rays "A" and "B" shown in Fig. 3 trace the limiting paths for light traveling from the line edge and reflecting off a flat piece of media into the camera's wide open aperture stop. Quite readily we see that the image formed of the object space line edge is the reimaging of the summation of those light rays over some aperture size on the flexible media mirror. The larger this mirror reflective aperture is, the less fidelity one obtains when observing localized changes in angularity of the media due to standing wave dynamics. We have termed this reflective aperture the "Mode Observer Reflective Blur Aperture."

For a flat piece of media and using the geometry of Fig. 3, one finds that this blur aperture is a function of the camera's aperture stop size (AS) and the ratio of object space distances s_{mp} and s_{cm} (s_{cm}/s_{mp}). S_{mp} being the distance from the media to the mode pattern and s_{cm} being the distance from the camera lens to the media. The width of the "reflective blur aperture" as shown in Fig. 3 has the following functional relationship:

$$Blur_{aperture} = \frac{AS}{1 + {Scm}/{Smp}} \tag{4}$$

where AS (mm) is the camera aperture stop diameter.

From this relationship one learns that to make measurements using this technique in the most effective manner it is important to have as bright of backlighting as possible for the structured mode pattern such that the camera's F# can be made as slow as possible (small AS). A secondary benefit of this high F# is reduced spherical aberration and improved depth of field. We also recognized from Eq. 4, that placing the structured mode pattern close to the media relative to the distance of the media from the camera reduces the blur aperture. Use of beam splitting optical configurations would enable the increase of this ratio (scm/smp) from 1 as was used in our tests.

Figure 7 plots the media "Reflective Blur Function" as described by Eq. 4. One will see noted on this figure the operation point of the system described in this paper. Based on a 16 mm camera lens focal length, an object space ratio of 1 (scm/smp) and an F# setting of 16, we find the media $Blur_{aperture}$ is on the order of 0.5 mm for our measurements. This appears to be an acceptable operation point based on the agreement between the estimated media Z deflection calculated from radial angular slope of the media as measured by the "Flexible Media Mode Observer" and actual measured Z deflections of the media during the testing. These results are reviewed in the Results and Discussion portion of this paper.

Electro-optical System Enhancement

It must also be remembered that standing wave instabilities having fundamental frequencies of greater than the video frame rate of the system (30 Hz) will appear as a blurred edge in captured frames. The implementation of a higher frame rate camera or a high scan rate line sensor would enable the researcher to investigate these dynamics more thoroughly, but consideration for minimizing the reflective blur function will require such a system to have proportionately brighter back-

lighting. Strobe lamp techniques could possibly be used to lock in visually to these higher frequency instabilities in the standing waves structure as well.

RESULTS AND DISCUSSION

To obtain the actual displacement map of the disk, one has to integrate the slope profile over the entire disk surface which can only be feasible with digital image grabber and extensive computer image processing capability. An alternate method is to examine the displaced profile along certain radial lines which is much less involved. This latter approach is adopted here to demonstrate the quantification of the mode observer results.

In particular, the displacement along two specific radial lines are calculated. One is the radial line that passes through the trailing edge of the slider, the other through the intersection of HSA arm and disk outer periphery upstream of the slider. The cases of larger head access slot with head penetration changes are studied for disk rotational speeds of 3000 rpm and 4500 rpm. Figures 8 and 9 show the mode observer image of disk deflections for these conditions (from Fig. 3 and 4 of Ma and Jones). The radial lines where quantifications are performed are also highlighted. Figures 10 and 11 are the results of these quantifications.

To obtain displacement, one had to measure the distance between the undistorted and distorted target circles along the radial line. That distance multiplied by a slope factor represents the angular distortion of the media at the location where the radial line intersects with the distorted target circle. This explains why the data points on Figures 10 and 11 have different radii. The displacement at each data point is calculated using a simple averaging method.

Closer examination of Fig. 10 shows that at head penetration of -.3 mm and 3000 rpm, the disk at the head is about .3 mm below nominal plane. As the head penetration increases to 0 and then on to .3 mm, the disk at the head does not move up by the same amount as the head penetration change. This indicates that both the head and media control the resultant location of the head disk interface plane. Secondly, there exists a strong bias, such that the disk tends to not follow the head with positive penetration. This probably is the result of the formation of the downward facing umbrella mode which resists the upward movement of the disk. It is also noticed that the disk deflection upstream of the heads along the arm radial line experienced minimal changes. This further indicates the existence of the resistance of the disk to upward movement.

Figure 11, on the other hand, shows a much more drastic disk movement. At Z=-.3 mm, disk displacement along the head appears to be similar to that at 3000 rpm. The displacement along the arm line is slightly upward. As the head penetration increases to 0 mm, the disk along both radial lines moves up; however it is more prominent along the head line. At Z= .15 mm, the disk was moved up along the head line but had a sudden drop along the arm line. This, as seen from Fig. 9, is the result of disk snap. At Z of .3 mm, the disk along the two radial lines moves in the opposite direction even further as the disk experienced another snap. This example illustrates the advantage of the Mode Observer over other existing techniques very well, since the result of Fig. 11 would be very difficult to explain without knowing the overall disk deformation.

CONCLUSIONS

The "flexible disk mode observer" instrument was examined in detail as an optical instrument. The angular deflection conversion factor was derived such that one can calculate the angular deformation of the disk from the displacement of the "structured mode pattern." The spatial resolution of the instrument was obtained as well as methods of improving the instrument through the aids of the "Blur Function."

The cases studied showed that both the disk and heads control the flying characteristics of the head to disk interface. They also indicated the strong downward facing bias of the rotating flexible disk. These studies further demonstrate the advantages of the "Flexible Disk Mode Observer" technology over other measurement methods due to its ability to provide the researcher with real time topographic information as to the dynamic mode structure of the entire disk as well as provide a means to quantify this data. The ability to observe standing wave mode snapping as a function of various system parameters changing, illustrates one of the critical insights this instrument provided the Zip design team.

ACKNOWLEDGMENTS

The authors would like to thank our colleages at Iomega who in various ways contributed to this work. These would include Dave Jones, Jim Bero, Brent Watson and Bob Bruce. Also, we would like to take this opportunity to thank George Krieger who for the past two years has been a dynamic or more apply a "Just Do It" Senior Director of New Product Development as he moves to his new assignment.

REFERENCES

Lamb, H. and Southwell, R.V., 1921, "The Vibration of a Spinning Disk," Proceedings of Royal Society of London, Series A, Vol. 99, pp. 272-280.

Southwell, R.V., 1921, "On the Free transverse Vibrations of a Uniform Circular Disc Clamped at its Center; and On the Effects of Rotation," Proceedings of Royal Society of London, Series A, Vol. 101, pp. 133-153.

Benson, R.C. and Bogy, D.B., 1978, "Deflection of a Very Flexible Spinning Disk Due to a Stationary Transverse Load," ASME Journal of Applied Mechanics, Vol. 45, No. 3, pp. 636-642.

Benson, R.C., 1983, "Observations on the Steady-State Solution of an Extremely Flexible Spinning Disk with a Transverse Load," ASME Journal of Applied Mechanics, Vol. 50, No. 3, pp. 525-530.

Ono, K. and Maeno, T., 1986, "Theoretical and Experimental Investigation on Dynamic Characteristics of a 3.5 inch Flexible Disk Due to a point Contact Head," Tribology and Mechanics of Magnetic Storage Systems, Bhushan, B, and Eiss, Jr., N.S., ed., STLE Park Ridge, IL, SP-21, pp. 144-151.

Adams, G.G., 1987, "Critical Speeds for a Flexible Spinning Disk," International Journal of Mechanical Sciences, Vol. 29, No. 8, pp. 525-531.

Adams, G.G., 1980, "Analysis of the Flexible disk/Head Interface," Journal of Lubrication Technology, Vol. 102, No. 1, pp. 86-90.

Greenberg, H.J., 1978, "Flexible disk-Read/Write Head Interface," IEEE Transactions on Magnetics, Vol. 14, No. 5, pp. 336-338.

Kitagawa, K., Ohashi, H., and Imamura, M., 1990, "Head-to Disk Interface in a Rapidly Rotating Flexible Disk Using Flying Heads", Tribology and Mechanics of Magnetic Storage Systems, Bhushan, B, and Eiss, Jr., N.S., ed., STLE Park Ridge, IL, SP-29, pp. 49-54

Carpino, M. and Domoto, G.A., 1988, "Investigation of a Flexible Disk Rotating near a Rigid Surface," Journal of Tribology, Vol. 110, No. 4, pp. 664-669.

Ma, Y. and Jones, D.E., 1995, "A Qualitative Experimental Investigation of Flexible Media Dynamics," 1995 ASME International Mechanical Engineering Congress and Exposition, Advances in Information Storage and Processing Systems - 1995, pp. 283-292.

Thomas, F., 1993, "Manufacture of 21 MB Floptical disk using acousto-optically controlled laser ablation process," SPIE Proceedings Vol. 2062, Lasers as Tools for Manufacturing, [2062-15].

APPENDIX A - FIGURES

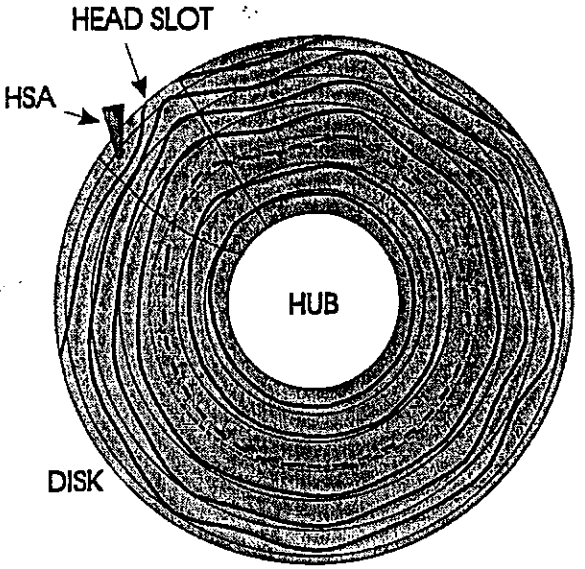

FIG. 1 TYPICAL ZIP FLEXIBLE MEDIA STANDINGWAVE TOPOGRAPHY

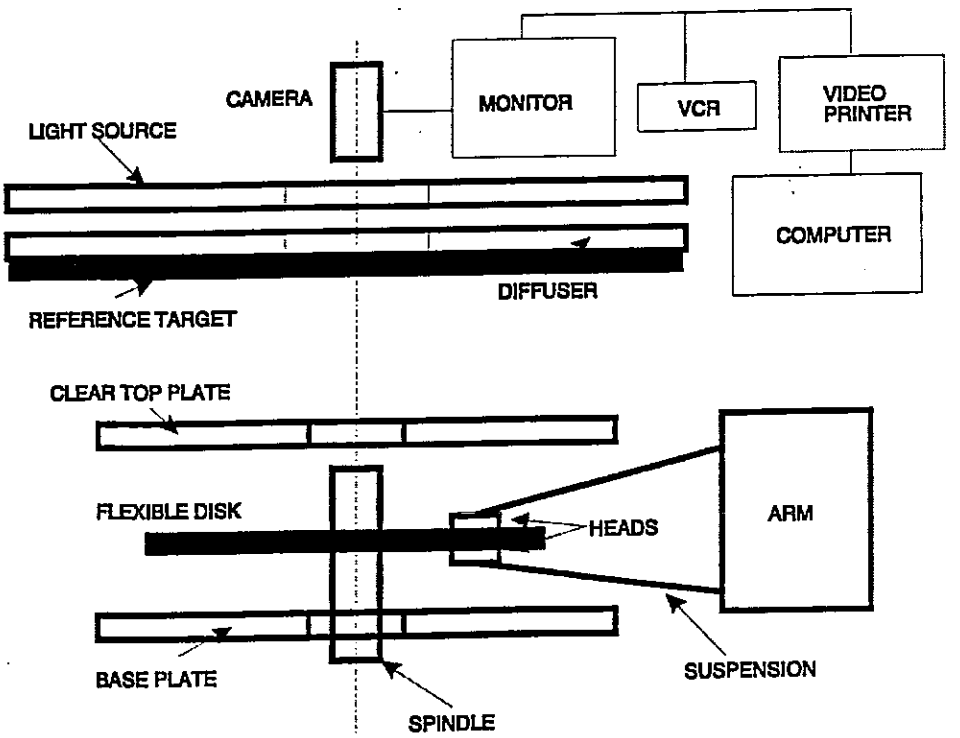

FIG. 2 "FLEXIBLE DISK MODE OBSERVER" BLOCK DIAGRAM

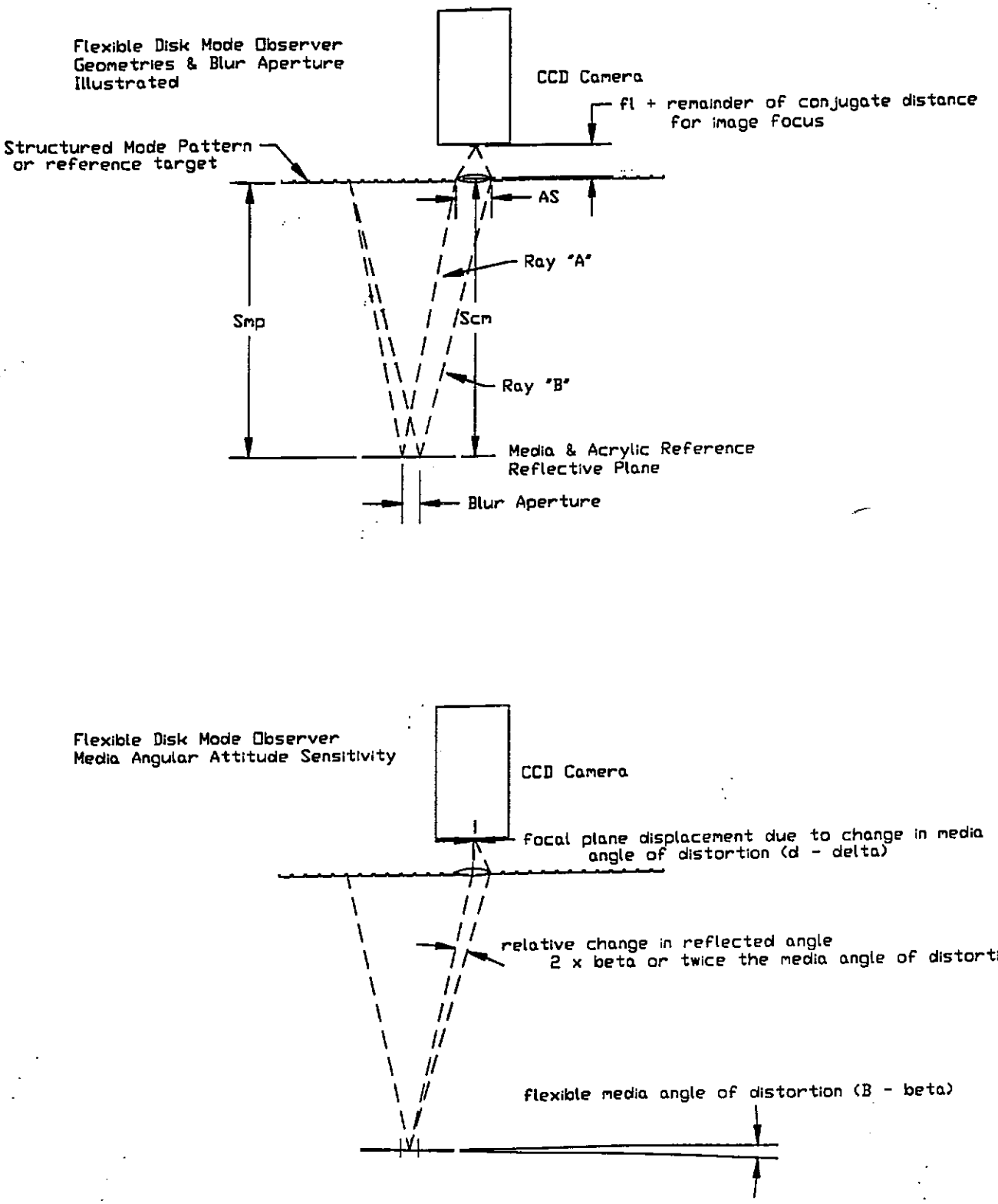

FIG. 3 OPTICAL LAYOUT OF "FLEXIBLE DISK MODE OBSERVER"

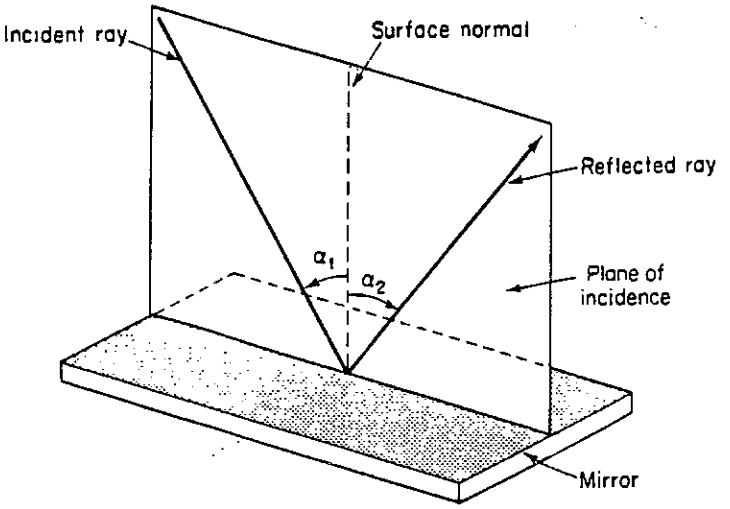

FIG. 4 FERMAT'S LAW OF REFLECTION ILLUSTRATION

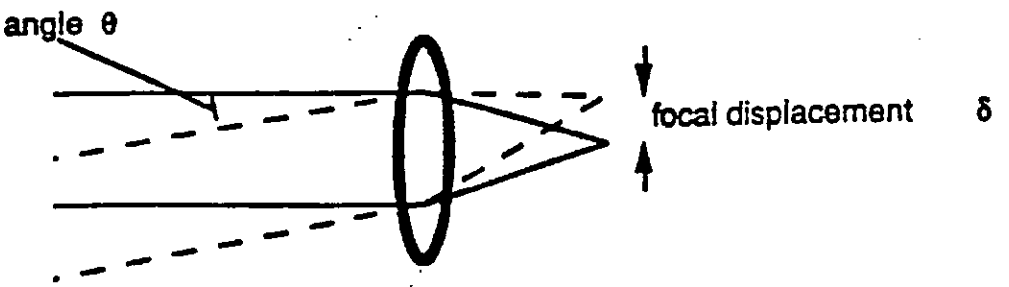

FIG. 5 STRUCTURED LINE EDGE DISPLACEMENT IN FOCAL PLANE

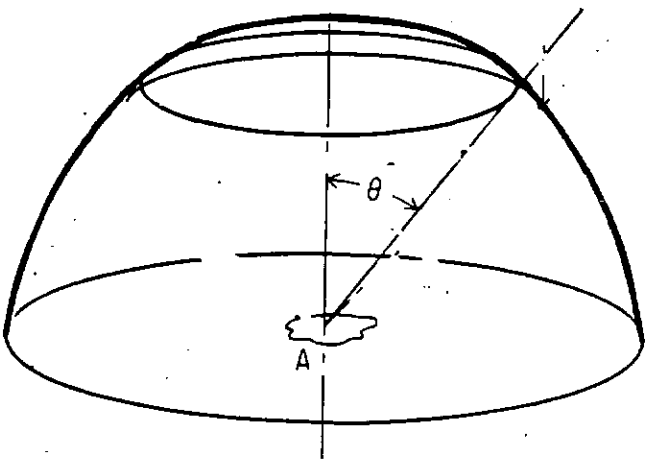

Irradiance from the Structured Mode Pattern is Lambertian and as such its' intensity in any direction is proportional to the cosine of the angle θ shown in this figure.

FIG. 6 LAMBERTIAN LIGHT SOURCE INTENSITY PROFILE

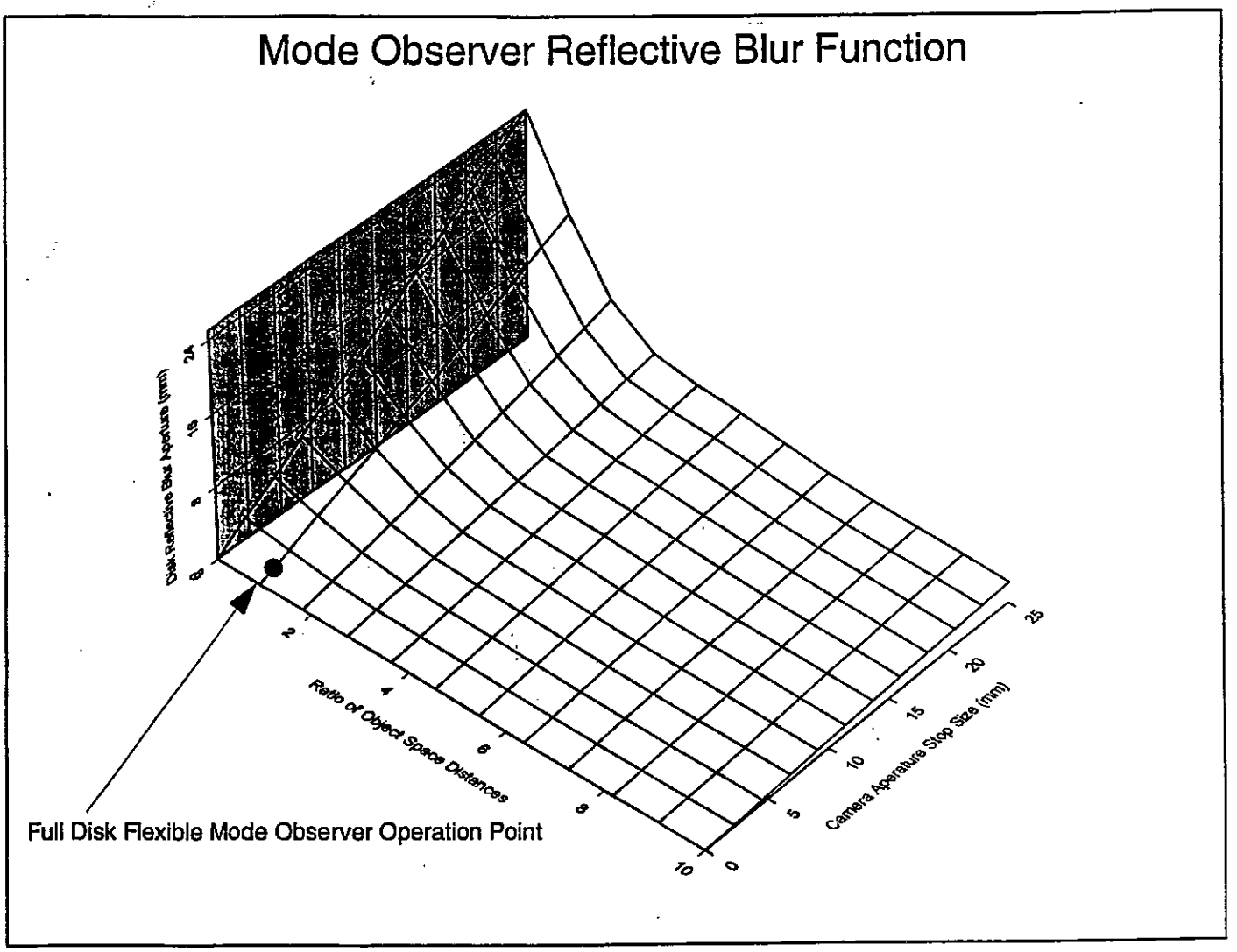

FIG. 7 MODE OBSERVER REFLECTIVE BLUR FUNCTION

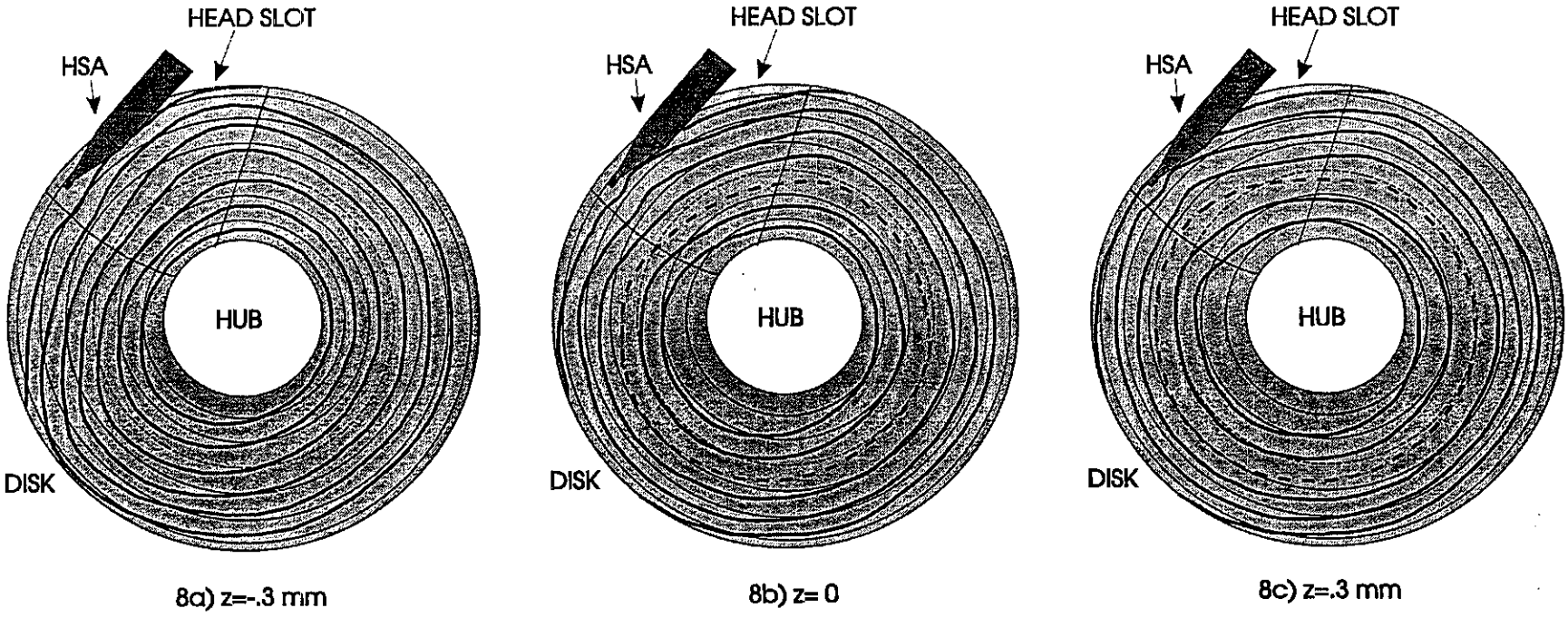

8a) z=-.3 mm

8b) z= 0

8c) z=.3 mm

FIG. 8 DISK DEFLECTIONS AT 3000 RPM

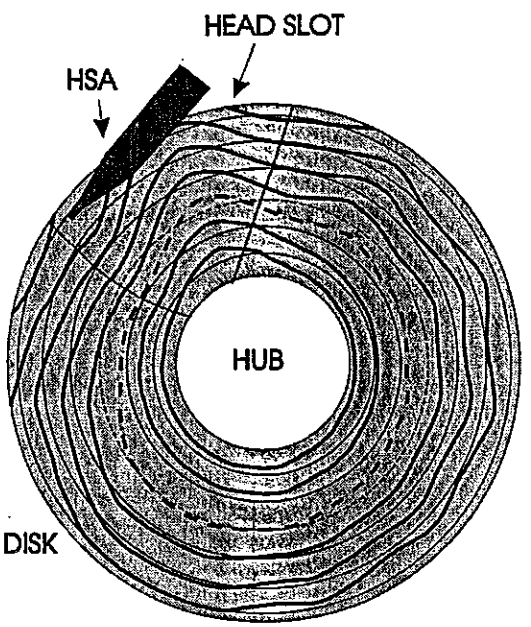

9a) z= -.3 mm

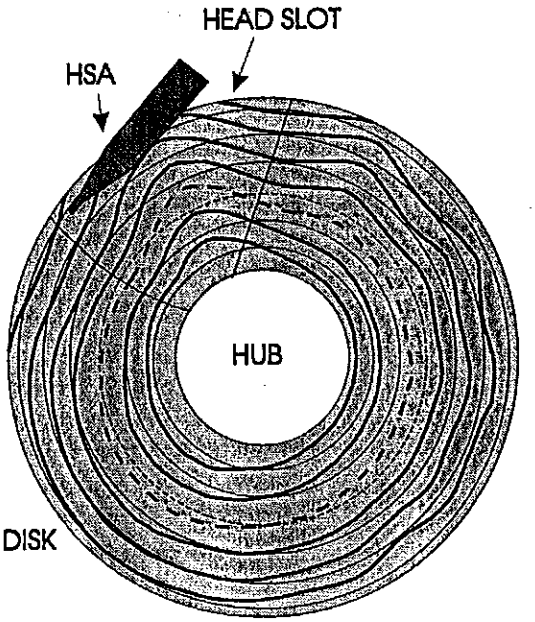

9b) z= 0

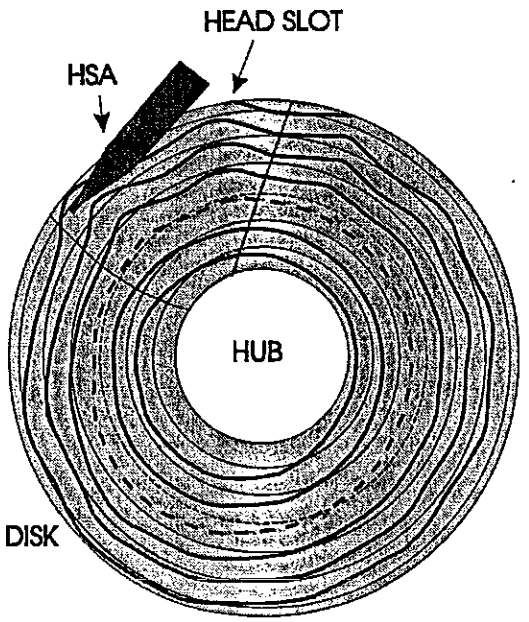

9c) z=.15mm

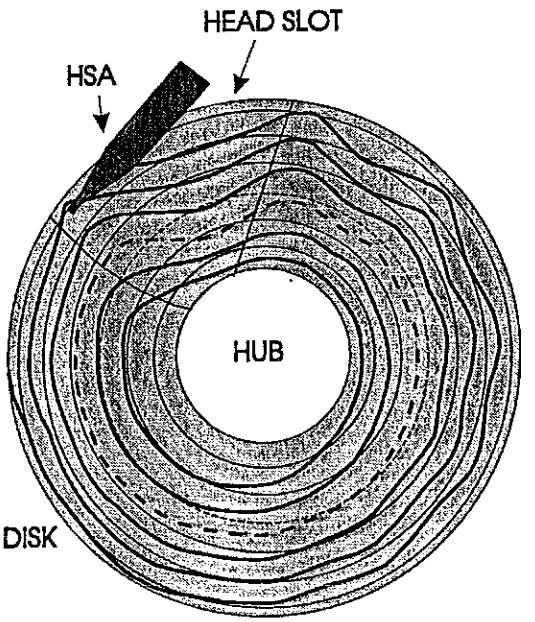

9d) z= .3mm

FIG. 9 DISK DEFLECTIONS AT 4500 RPM

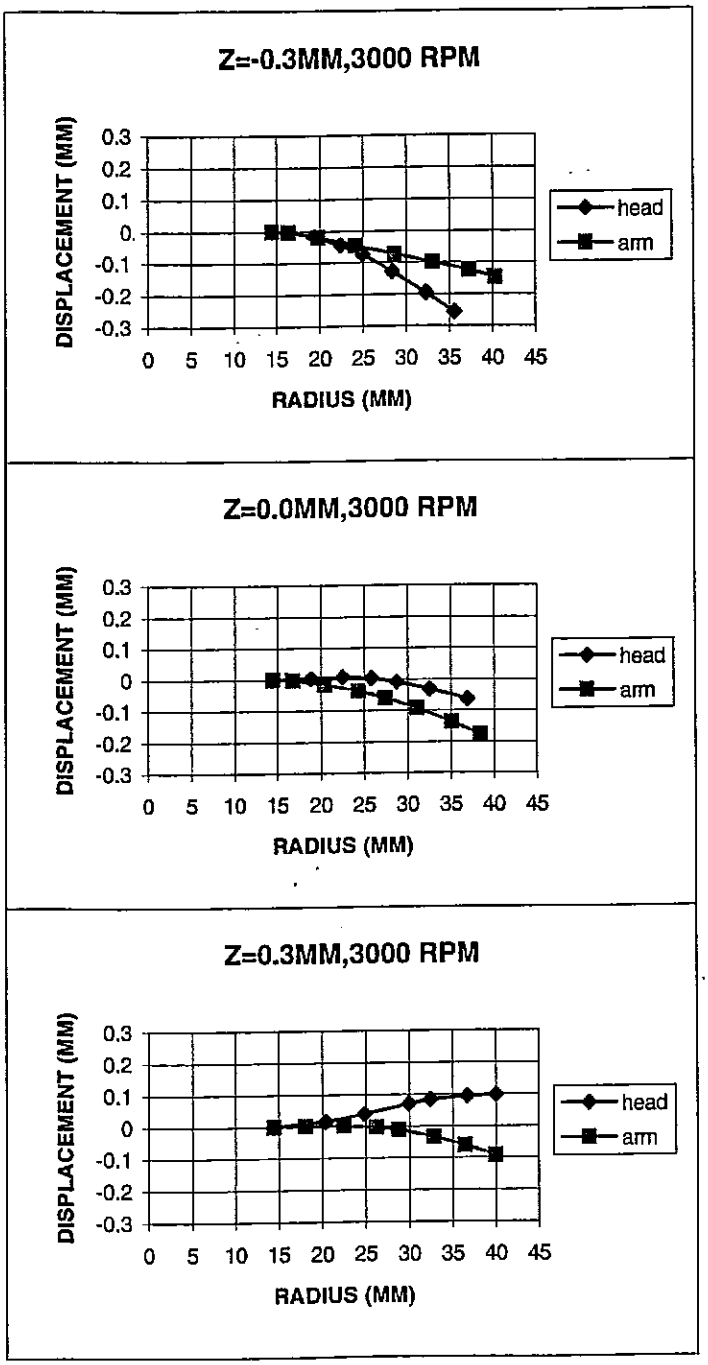

FIG. 10 CALCULATED DISK DISPLACEMENT AT 3000 RPM

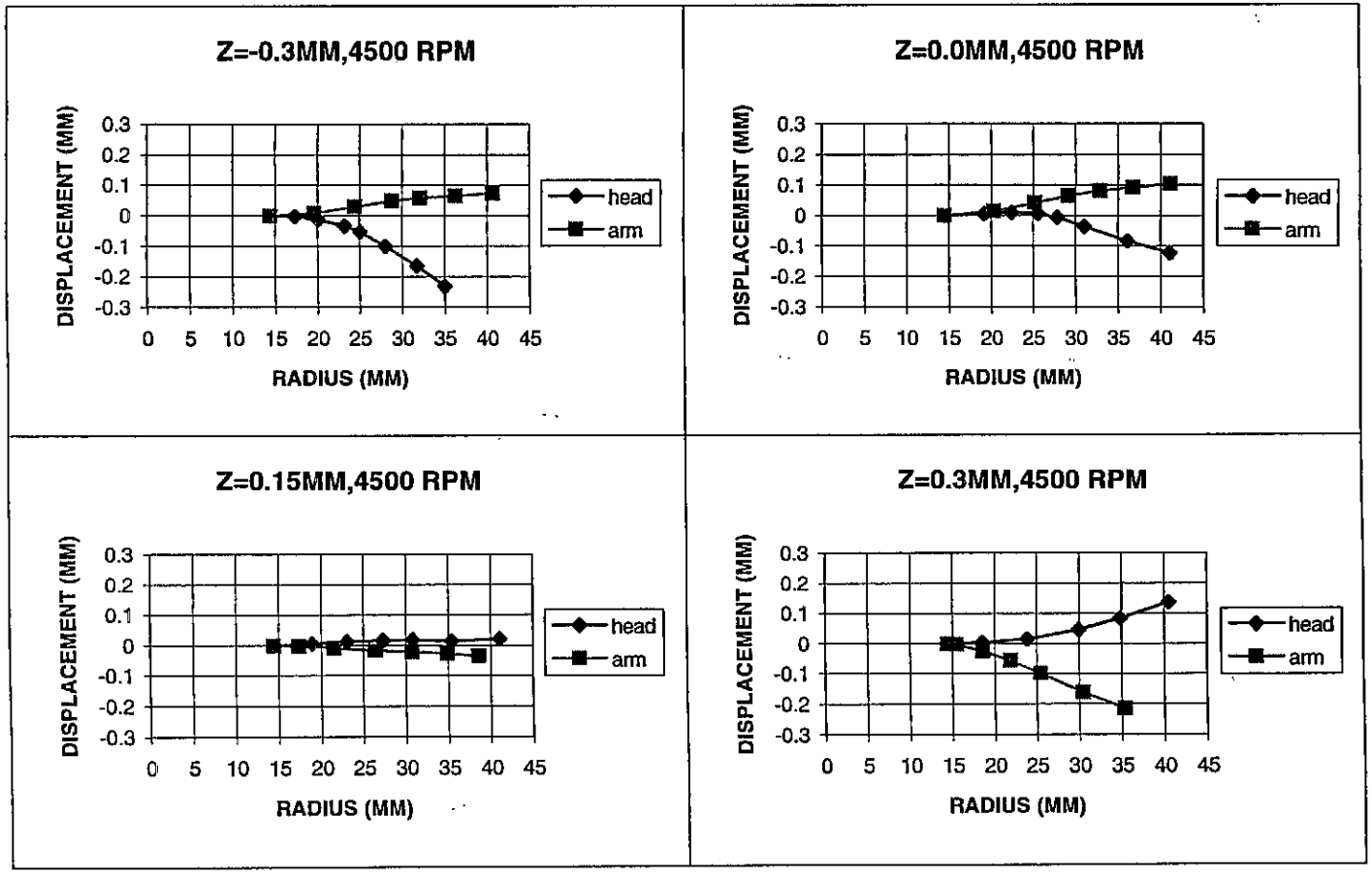

FIG. 11 CALCULATED DISK DISPLACEMENT AT 4500 RPM